Modification of SiO through room-temperature plasma treatments, rapid thermal annealings, and laser irradiation in a nonoxidizing atmosphere

F. Rochet
Groupe de Physique des Solides de l'ENS, Université Paris VII, Tour 23, 2 Place Jussieu, 75251 Paris Cédex 05, France

G. Dufour and H. Roulet
Laboratoire de Chimie Physique, Université Pierre et Marie Curie, 11 Rue Pierre et Marie Curie, 75231 Paris Cédex 05, France

B. Pelloie and J. Perrière
Groupe de Physique des Solides de l'ENS, Université Paris VII, Tour 23, 2 Place Jussieu, 75251 Paris Cédex 05, France

E. Fogarassy and A. Slaoui
Centre de Recherches Nucléaires, Laboratoire PHASE, 23 Rue du Loess, 67037 Strasbourg Cédex, France

M. Froment
Physique des Liquides et Electrochimie, Université Pierre et Marie Curie, Tour 22, 4 Place Jussieu, 75230 Paris Cédex 05, France
(Received 29 June 1987)

We have studied the modification of *a*-SiO thin deposited films through Ar-plasma treatment at room temperature, through heating (rapid thermal annealing), or through irradiation (uv-laser treatment), in a nonoxidizing atmosphere. Rutherford backscattering spectroscopy, reflection high-energy electron diffraction, ir-absorption, and x-ray photoelectron spectroscopy techniques have been used in combination to investigate the atomic composition and the structural and chemical nature of SiO films after various nonoxidizing treatments. We show that the as-deposited oxide is not a mixture of Si and SiO_2 and separates into phases as a result of processing. The effects of irradiation by low-energy electrons at room temperature (plasma treatment) are similar to those observed for high-temperature treatments. A possible microscopic mechanism, leading to silicon cluster growth, is proposed to explain the transition from a material rich in intermediate suboxides (as-deposited SiO) to the mixture structure (phase-separated Si and SiO_2).

INTRODUCTION

Interest in the oxidation of silicon monoxide (SiO) into SiO_2 has been recently renewed for both practical[1] and more fundamental reasons, as SiO is believed to be present as an intermediate reactive layer between the silicon substrate and thermally growing SiO_2 films.[2,3] The structure and physico-chemical properties of this transition region are still open questions. Therefore, the SiO thin film can be used as a model system for the Si-SiO_2 interface. More especially the behavior of this metastable compound during its oxidation into the dioxide deserves interest. As a result, the possibility of converting silicon monoxide into the dioxide has been checked by various methods, and the first step leading to the oxidation of SiO thin films during oxygen plasma anodization,[4] rapid thermal annealing,[5] or pulsed excimer uv laser irradiation[6] in an O_2 atmosphere is generally considered to be the macroscopic reaction

$$2\ \mathrm{SiO} \rightarrow \mathrm{SiO_2} + \mathrm{Si} \quad (1)$$

where simultaneously silicon dioxide is formed, and Si atoms are liberated and oxidized in a second step.

Our aim in this work is to give a more microscopic insight into the first step of SiO oxidation, i.e., into the transformation (1). So, we have studied the structural and chemical changes induced by the electronic flux during plasma treatment at room temperature, by heating or uv irradiation in the absence of the oxidation phenomenon.

The macroscopic reaction (1) corresponds to the transition between the two extreme descriptions of the SiO films, i.e., the random-bonding model proposed by Philipp[7] and the mixture model. At a microscopic level, atomic and/or ionic migrations are needed to achieve such a transition, and our purpose is to propose a microscopic mechanism for the creation and the movement of the migrating species leading to phase separation in SiO, by the growth of Si clusters in an SiO_2 matrix.

EXPERIMENT

Sample preparation and treatments

100-nm-thick SiO films were deposited on (100)-oriented Si substrates, kept at room T, by evaporation of high-purity commercial SiO powder (grains, ~ 0.3 mm), the deposition rate being 1 nm s^{-1}. Composition and properties of such films strongly depend on the conditions under which the deposition is carried out, especially the substrate T.[8] Indeed it has been shown that for substrates kept at low temperatures, Si and O atoms tend to be randomly distributed in an amorphouslike medium, while under high temperatures they tend to separate into Si and SiO_2 phases. In our conditions, the as-deposited silicon monoxide films appeared to be composed of intermediate SiO_x forms and thus can be extensively described in the frame of a quasirandom-bonding model (see later).

Three kinds of treatments were then performed.

(i) *Argon-plasma treatments in a multipolar plasma set-up.*[9] This plasma source, which combines a hot-electron emitter and surface magnetic confinement, leads to homogeneous cold and dense (10^9–10^{10} cm^{-3}) discharges at very low pressure (5×10^{-4} Torr). Argon plasma treatments were performed at a constant regulated temperature (25 °C) which was measured on the back of the sample. The SiO films were biased with respect to the plasma, and as a result, an electronic current (10 mA/cm^2 constant current density) flows through the sample. The treatment time varies between 30 min and 10 h. When the sample is biased, a potential drop (ΔV) is established across it:

$$\Delta V = V_a - V_s ,$$

where V_a is the measured potential at the back of the sample and V_s is the surface potential, which depends only on the plasma parameters and current density. From this potential drop, an electric field is derived in the silicon monoxide. The value of the macroscopic field that drives the electrons across the oxide is around 3×10^6 V/cm.

(ii) *Rapid thermal annealing (RTA) in a flowing Ar atmosphere at 1100 °C for 5 sec (using tungsten halogen lamps as heating source).* When performed in oxygen this treatment leads to the conversion of SiO into SiO_2,[5] while in a neutral atmosphere, oxygen atoms are not incorporated.

(iii) *Laser irradiations in a neutral atmosphere (N_2 gas).* An ArF pulsed excimer laser was used (photon wavelength $\lambda = 193$ nm) with an energy deposition of 110 mJ/cm^2 per pulse, and 10^4 repetitions. In this treatment, specific photonic processes are expected, but owing to the high absorption coefficient of SiO for UV light, surface heating may also result from the uv-photon–solid interactions. Previous calculations have shown that the surface temperature of the sample could rise up to ~ 1100 C,[6] and thus the heating contribution cannot be neglected in such conditions.

For the rest of this article, the sample denomination will be simply "plasma," "RTA," and "laser" samples. The untreated one will be called "test" sample.

Sample analysis

Rutherford backscattering spectrometry (RBS)

The stoichiometry of the silicon oxide thin films was checked before and after the various treatments by Rutherford backscattering techniques in channeling geometry using ^4He particles with an incident energy of 1.8 MeV. In some cases backscattered particles were analyzed in glancing exit mode ($\theta_{lab} = 100°$) in order to increase the depth resolution in the region close to the very surface.

Reflection high-energy electron diffraction (RHEED)

The crystallographic structure of the near-surface region of the oxide films was investigated by RHEED at grazing incidence. The acceleration voltage of the electrons was 100 kV.

ir absorption

The samples have been characterized, at room T, by infrared absorption spectroscopy using a Perkin-Elmer 938G double-beam grating spectrometer. The widths and positions of the Si-O vibrational bands around 1000 cm^{-1} are strongly influenced by the bonding character, stoichiometry, density, and porosity of the Si-oxide films. Thus the transformation of the test sample by the various treatments was followed by investigating the spectral position of the Si-O vibrational stretching band, as well as its width at half maximum.

X-ray photoelectron spectroscopy (XPS)

X-ray photoelectron spectroscopy was used to investigate the electronic structure of the core levels and the valence band of the samples. The spectrometer used in this work was equipped with both a standard and monochromatized x-ray source (Al $K\alpha_{1,2}$, $h\nu = 1486.6$ eV). The photoelectron spectra using monochromatized radiation were scanned for Si $2p$ and O $1s$ levels with a total instrumental broadening of 0.55 eV.

The Si $2p$ line is actually a doublet with components Si $2p_{1/2}$ and Si $2p_{3/2}$ separated by 0.6 eV. In order to reduce the broadening of the spectra we removed the Si $2p_{1/2}$ components (for the substrate and the various oxidation states) by using the method developed by Nyholm and Mårtensson.[10] Such a numerical treatment can reveal small structures, formerly hidden by the Si $2p_{1/2}$ peaks. The valence-band spectra were also obtained with the monochromatized x-ray source but with an exit slit larger than in the case of Si $2p$ and O $1s$ spectra, in order to avoid prohibitive accumulation times. This is of course at the expense of the instrumental broadening (~ 1.5 eV). In all cases, the background was removed by using a program based on a nonlinear background-subtraction method.[10] The zero of the binding-energy scale was determined from the Fermi cutoff of a thick metal layer. No charging effects have been observed during the experimental runs.

Only the near-surface region of the oxide films (~ 10 nm) was studied by this technique, and since chemical or ion-beam etching may induce large modifications of the surface, we did not try to carry out an in-depth analysis.

RESULTS

RBS analysis

RBS was carried out to characterize the composition of the oxide films, and Fig. 1 shows a typical spectrum recorded in channeling geometry on the 100-nm-thick test sample. The ratio of the shaded areas labeled Si and O, when corrected for the differing relative Rutherford cross sections, gives the stoichiometry of the films. For the various samples, we found $(O)/(Si)=1.00\pm0.04$. None of the treatments resulted in an overall change in composition. The oxygen content of the samples was measured with nuclear reaction analysis, using the $^{16}O(d,p)^{17}O^*$ reaction, and within the $\pm 3\%$ precision of the experiments, no modification in the oxygen content was observed. To improve the precision of the stoichiometry measurement in the near surface region, RBS analyses in the glancing exit mode were carried out at a detection angle $\theta_{lab}=100°$. In these experimental conditions, the outgoing path of the backscattered α particles is greater (factor ~ 5) than standard 165° detection, leading thus to a magnification of the near surface region. Fig. 2 represents the front edge of the RBS spectra of the test and RTA samples in these conditions. Both spectra are directly superimposed showing the absence of formation of a thick SiO_2 surface layer. For the purpose of comparison, the spectrum of 13-nm-thick SiO_2 layer (obtained by plasma anodization) on SiO is also presented and it shows the presence of a plateau characteristic of SiO_2 (the spectrum of a pure thermal SiO_2 is also shown in Fig. 2) From the comparison of these spectra, the thickness of a topmost SiO_2 layer, if present on the RTA sample, should be very small. An upper limit thickness was estimated to be about 4 nm (from values of the stopping powers in the framework of the so-called "linear approximation"[12]).

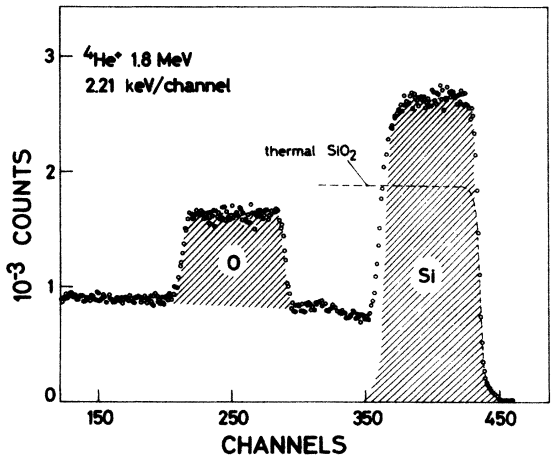

FIG. 1. RBS channeling spectrum for the 100-nm-thick "test" sample taken at a detection angle $\theta_{lab}=120°$.

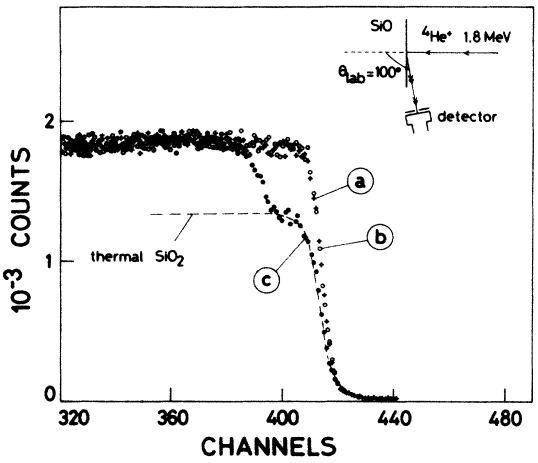

FIG. 2. RBS analysis in the glancing exit mode ($\theta_{lab}=100°$) of curve *a*, the test sample, and *b*, the RTA sample, and curve *c*, a 13-nm-thick SiO_2 layer on top of a SiO film.

RHEED analysis

The test sample gives diffuse rings characteristic of a highly disordered amorphouslike material. In contrast the plasma [Figs. 3(a) and 3(b)], RTA [Fig. 3(c)] and laser samples [Fig. 3(d)] exhibit, over the diffuse background of an amorphous matrix, bright points distributed on rings. The corresponding interreticular distances can be attributed to the presence of silicon microcrystallites. All the allowed reflections are present. No reinforcement along a given direction can be seen, thus the Si microcrystals are randomly oriented relative to each other in the oxide and also with respect to the substrate orientation. In addition, a few extra rings, that can be attributed to crystalline forms of silica, are seen in all the treated samples.

In the RTA and laser samples, the Si microcrystals seem to be homogeneously distributed with depth since no significant change was observed when the incident of the electron beam was modified. When the surface of the plasma sample is observed at a very glancing incidence [Fig. 3(a)], the RHEED patterns are essentially composed of bright points which correspond to a Si crystallites. At a less glancing incidence, the film is observed more in-depth [Fig. 3(b)] and over the strong "amorphous" background, rings corresponding to crystalline-silica now become visible, with the following interreticular distances (d_{hkl}): 0.337, 0.268, 0.225, 0.216, 0.203, and 0.178 nm. These d_{hkl} could be attributed to coesite or β-quartz. This suggests that Si microcrystallites are preferentially located near the external surface.

Thus, whatever be the treatment, a transformation in the structure of SiO is evidenced by RHEED: Si microcrystallites (the size of which varies from 10 to 100 nm) are formed, embedded in an amorphous matrix. While under heat treatments the growth of Si crystallites was already reported,[13] these RHEED observations show the formation of crystalline Si areas under plasma treatments at room *T*. Moreover, in the same conditions, crystalline silica areas are also formed during the SiO transformation.

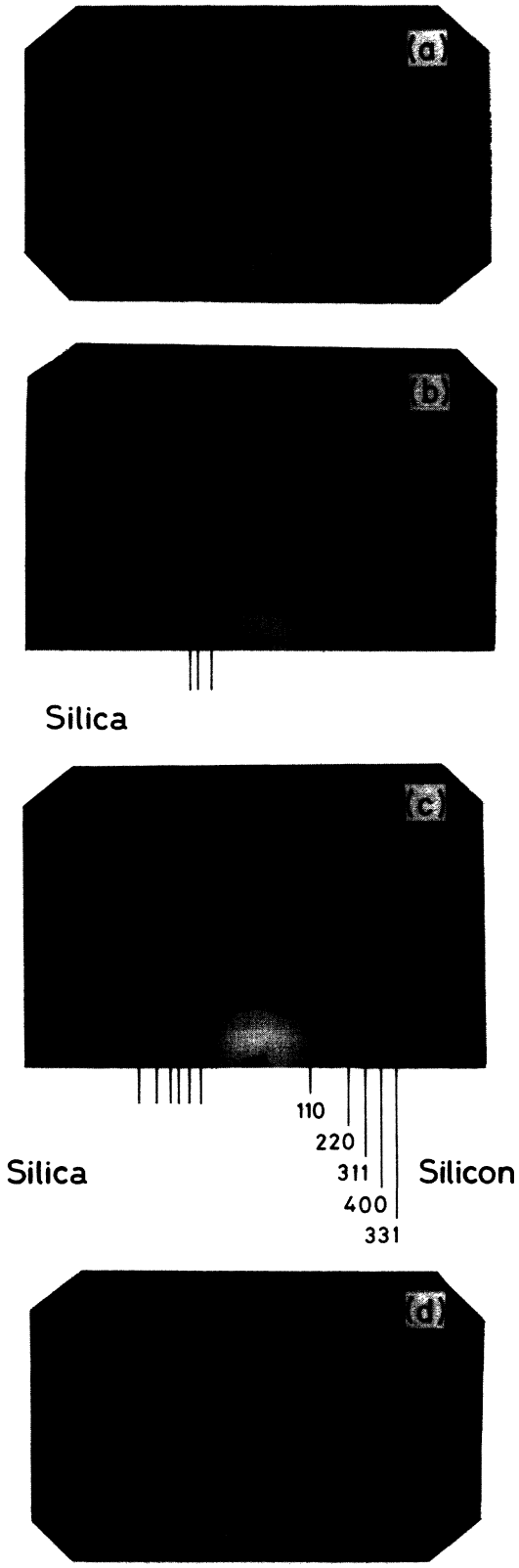

FIG. 3. Electron diffraction patterns observed by reflection (RHEED): (a) plasma sample (surface observation), (b) plasma sample (in-depth observation), (c) RTA sample, (d) Laser sample. Bright points distributed on rings corresponding to *c*-Si interreticular distances are seen in (a)–(d). Rings indicative of an ordered SiO_2 phase are seen in (b) and (c).

ir-absorption analysis

The ir-absorption band in the 950–1100 cm^{-1} frequency range related to the Si-O stretching mode is presented in Fig. 4 (test and plasma sample) and Fig. 5 (test, laser and RTA sample). In the case of the as-deposited SiO films, the characteristic peak is located around 980 cm^{-1}. It has been previously shown,[14] that the frequency of the Si-O stretching vibration depends on the oxygen atomic composition, i.e., on x in the formula SiO_x. It increases from $\sim$940 cm^{-1} for oxygen traces in Si network to about 1080 cm^{-1} for $x=2$ (pure thermal SiO_2) with a rather linear variation, the frequency for stoichiometric SiO lying around 1000 cm^{-1} as it is observed in this work. SiO films evaporated at high deposition rates (high substrate T) exhibit Si-O stretching modes at higher frequencies. This is indicative of a mixture of Si and SiO_2. In contrast, the spectra of the as-deposited SiO films shown here, are rather characteristic of a material without phase separation.

After plasma treatment, the ir peak is shifted towards 1050 cm^{-1}, in relation with changes in the chemical bonding. For the sake of comparison, we show also in Fig. 4 the ir-absorption spectrum recorded from a SiO sample anodized in oxygen plasma at room T up to the complete transformation of SiO into SiO_2. Both the ir peaks are located at the same frequency of 1050 cm^{-1}, different from that observed for thermal SiO_2 (1080 cm^{-1}). This means, firstly, that a chemical modification is induced in the SiO film by the plasma treatment, leading to the formation of SiO_2 regions, and secondly that this effect has not a thermal origin since the peak location is characteristic of SiO_2 grown at room T (by plasma anodization) and not of thermal SiO_2 formed at high T.

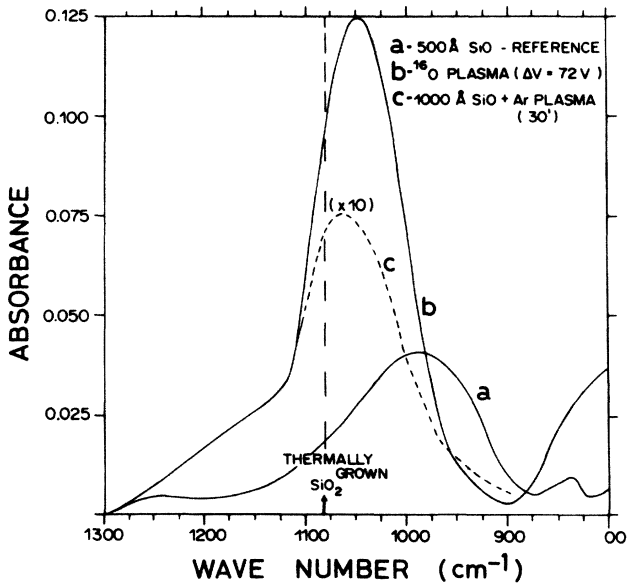

FIG. 4. ir-absorption spectra (Si-O stretching modes) of the samples kept at room temperature: *a* the test sample, *b* a SiO film oxidized in oxygen plasma, *c* the plasma sample (SiO film treated in Ar plasma).

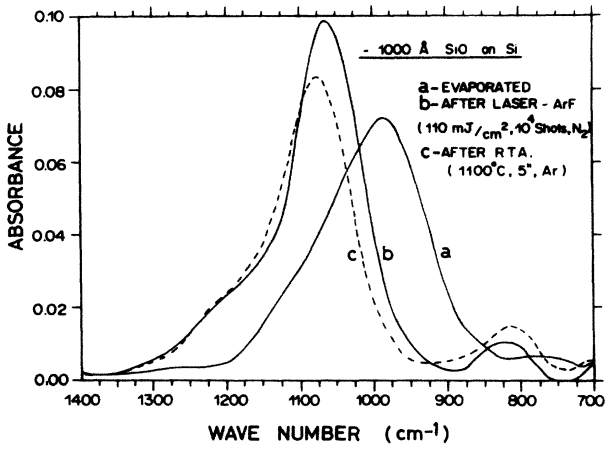

FIG. 5. ir-absorption spectra (Si-O stretching modes) of the samples treated at high temperature: *a* test sample, *b* laser sample, *c* RTA sample.

Figure 5 shows that the ir peak, corresponding to Si-O stretching mode after uv laser irradiation and rapid thermal annealing is located at the frequency (1080 cm^{-1}) expected for SiO_2 formation at high T. Here also, we conclude that silica regions are formed during these treatments. As the laser sample shows a band position characteristic of the thermal SiO_2, this also supports the thermodynamical calculations[6] indicating a large elevation of surface temperature during laser irradiation.

The comparison of Figs. 4 and 5 shows also that the width of the absorption band (FWHM) is significantly larger for the plasma sample (> 110 cm^{-1}) than for the high-T samples. As previously reported,[15] SiO_2 grown at low-T presents differences with respect to high-T silica in density, porosity, strains, etc which are evidenced by larger band width.

Thus, whatever be the treatment (high T or room T), the SiO layer, initially fairly homogeneous, has been modified since the existence of SiO_2 regions is clearly shown by ir absorption spectroscopy. The use of XPS is now necessary to monitor the evolution of the local chemistry in these layers, and more particularly the fate of the intermediary silicon oxides after treatment.

XPS analysis

Si 2p core-level spectra

The Si 2*p* lines after background subtraction and Si $2p_{1/2}$ stripping are shown in Fig. 6. These spectra will be interpreted in terms of the superposition of different chemically shifted components. Imagine we start with the *a*-Si network on which each atom is surrounded by four other Si atoms as nearest neighbors. Then, an increasing number of the homopolar Si—Si bonds re replaced by heteropolar Si—O bonds as oxygen is added to the network. The charge transfer for Si to the much more electronegative O leaves a positive charge on the Si atom, which results in a shift of all Si deep core levels towards higher binding energy. We thus expect five components Si^0, Si^{1+}, Si^{2+}, Si^{3+}, and Si^{4+}, corresponding to Si atoms where zero, one, two, three, or all four Si—Si bonds have been replaced by Si—O bonds.

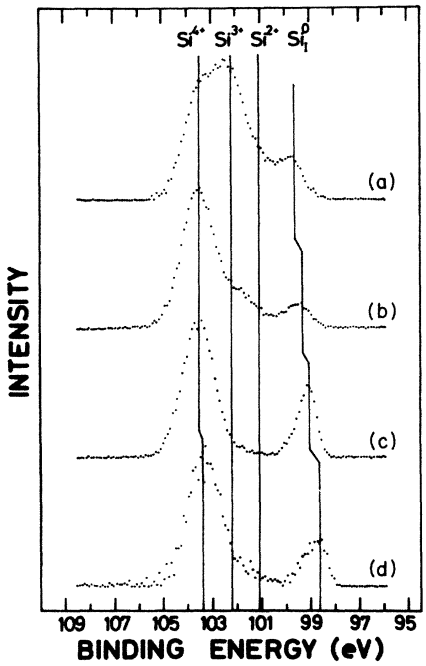

FIG. 6. Si 2*p* core level spectra after Si $2p_{1/2}$ stripping of the (a) test sample, (b) plasma sample, (c) RTA sample, and (d) "laser" sample. The energy positions of the lines attributed to the various oxidation states are indicated. The zero energy is taken at the Fermi level.

One can distinguish, even in the case of the "test" sample [Fig. 6(a)], the Si 2*p* line related to nonoxidized atoms from the contribution of Si atoms bonded to O atoms lying at higher binding energies. Moreover, the Si 2*p* lines of both the "oxide" and the "pure" silicon are not symmetrical: Contributions other than peaks whose centroids correspond to relative peak maxima are needed to explain this form. Therefore, the test sample spectrum clearly shows that the as-deposited SiO film is not a simple mixture of Si and SiO_2 because of the large contribution of suboxide states, although it contains a significant amount of Si bound only to other Si atoms. All the various treatments lead to a drastic decrease of the intermediary suboxide states: Si^{4+} in SiO_2 (at the highest binding energy) and Si^0 become the prominent lines, indicating that phase separation has greatly advanced, by the transformation of the metastable intermediate SiO_x forms.

The physical system which is the most comparable to ours is the *c*-Si/SiO_2 interface or the problem of the initial step of oxygen reaction on clean Si surfaces.[16–20] The Si 2*p* core levels of Si(111) surfaces exposed to oxygen were studied and the four oxygen-induced Si states were found with energy shifts towards higher binding energy, equal to 1.0, 1.8, 2.6, and 3.5 eV with respect to the substrate line.[16,17] These shifts, in this order, are considered to be the signatures of the four possible oxidation states of silicon, Si^+, Si^{2+}, Si^{3+}, and Si^{4+}. The energy shift per Si—O bond, which is constant and equal to 0.8

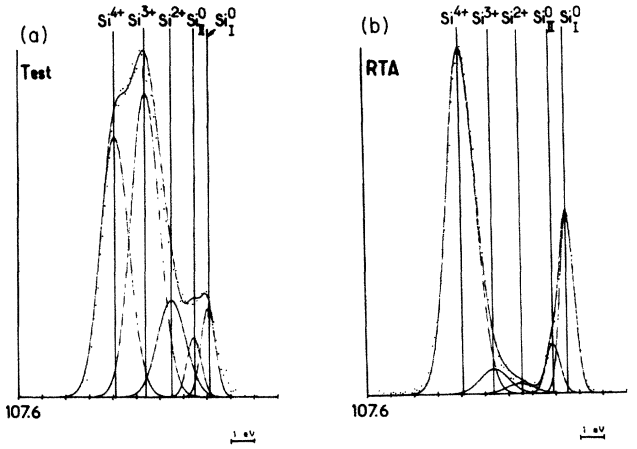

FIG. 7. Example of spectra reconstructed from a summation of Gaussians. We show the energy positions E_B at which the Gaussians are centered: (a) test sample, (b) RTA sample.

eV in Refs. 16 and 17, can attain 1.0 eV according to a recent report.[18] In the latter work, considering the very small oxide thicknesses involved (less than 0.7 nm), it is very hard to conclude that final-state effects (i.e., relaxation effects) can already be introduced to account for such small discrepancies. However, in the case of thicker films, the Si^{4+}-Si^0 shift can vary from ~ 3.6 to ~ 4.1 eV (Ref. 19) when the oxide is believed to recover its bulk properties. Similar observations were reported[20,21] and attributed to a modification of the extra atomic relaxation energy in the outer SiO_2 layers, "far" from the semiconducting substrate. Thus, large effects of final states on the measured binding energy are expected, as the core hole screening on a given Si atom is deeply affected by the scale on which a given homogeneous medium can extend.

Taking this into account, we have interpreted our Si $2p$ core level spectra in terms of a superposition of energy-shifted components corresponding to the four possible oxidation states of Si but with no *a priori* assumption on the energy shift per Si—O bond as discussed above. Due to the observed asymmetry, two lines (Si^0_I and Si^0_{II}) separated by 0.6 eV, were attributed to pure Si, the less intense one (Si^0_{II}) lying at higher binding energy. This line was previously interpreted[20] as due to Si atoms close to the Si-oxide interface. Here, these S^0_{II} might be considered to correspond to Si atoms close to the periphery of silicon clusters. We used a fitting procedure based on the summation of Gaussians whose width at half maximum (2Γ), position (E_B) and relative weight (W) can be defined to reconstruct the experimental spectra. Here we chose $\Gamma = 0.7$ eV for silicons bonded to oxygen, and $\Gamma = 0.35$ eV for silicon bonded only to silicon as in a preceding work,[20] in which the experimental conditions were exactly the same. Two illustrative reconstructions are given in Fig. 7 for two extreme cases, the test and the RTA samples, and the complete results are summarized in Table I; the positions of the various Si states are also indicated in Fig. 6 by solid lines. It appears that the three oxide lines we need to fit the spectra can be attributed to Si^{4+}, Si^{3+}, and Si^{2+} states. Remarkably, the oxide lines' binding energies are not affected by the treatments, while the two Si^0 lines go towards lower binding energies. The energy shift per Si—O bond is greater than in the c-Si/SiO_2 thin-films system. The relative weight of the Si^0_{II} state is also greater: that explains why no spin-orbit splitting is observable (spectra not shown here) in contrast to bulk crystalline silicon. Recall that the same observation is made for a-Si.[22]

The major effect of the treatments is to reduce the weight of the suboxide lines (Si^{3+}, Si^{2+}): For example, Si^{3+} is reduced from 42% in the test sample to $\sim 5\%$ in the RTA sample. It decreases to only $\sim 13-17\%$ in the case of the laser sample or of the plasma sample. As a result, the intensity of the Si^{4+} and Si^0 lines is increased, while the Si^{4+}-Si^0 shift is dependent on the sample treatment and can reach 4.75 eV in the case of laser irradiation.

In the random bonding model, Si—Si and Si—O bonds follow a statistical distribution deduced from the suggestion of Phillip,[7] who considers SiO_x as composed of tetrahedra of the type Si—(Si_y—O_{4-y}) arranged in a continuous random network. For $x = 1$ (i.e., SiO) the respective weights of the Si^0, Si^{1+}, Si^{2+}, Si^{3+}, and Si^{4+} are 0.0625, 0.25, 0.375, 0.25, and 0.0625. This cannot be accounted for by the reconstruction of the test sample spectrum we have made (Table I). The weight of the Si^0 states is too high compared to Phillipp's calculation. Thus,

TABLE I. Results of the fitting procedure of the Si $2p_{V2}$-stripped Si $2p$ spectra, i.e., binding energies (E_B), and relative weights (W). We give also the oxygen stoichiometry x one would have for a uniform in-depth composition of the layers.

		Test		Plasma		RTA		Laser	
Sample		E_B (eV)	W (%)	E_B (eV)	W (%)	E_B (eV)	W (%)	E_B (eV)	W (%)
Oxygen-induced states	Si^{4+}	103.5	35.2	103.5	66.7	103.5	70.9	103.4	67.0
	Si^{3+}	102.2	41.6	102.2	16.7	102.2	4.7	102.2	13.0
	Si^{2+}	101.1	12.8	101.1	8.0	101.1	1.6	101.1	4.0
Silicon states	Si^0_{II}	100.15	4.0	99.85	3.3	99.70	4.7	99.3	6.0
	Si^0_I	99.55	6.4	99.25	5.3	99.05	18.1	98.65	10.0
Si^{4+}-Si^0_I shift (eV)		3.95		4.25		4.45		4.75	
x		~ 1.5		~ 1.7		~ 1.5		~ 1.6	

despite the fact that the test sample is not a composite material consisting of two distinct phases, there is no complete agreement with the idealized random bonding statistics, since the XPS measurements reveal an appreciable mixture character. Indeed it is not so surprising to find a deviation from a pure statistical model which does not consider that SiO is thermodynamically unstable. This means that in the as-deposited material, there might already be a slight clustering of Si atoms during deposition.

After the various treatments, the transition from an intermediate oxides-rich system to a mixture system is indicated, although appreciable amounts of suboxide remain present. In the frame of the mixture description, only Si and SiO_2 clusters exist, and thus *a priori* only two kinds of tetrahedra with $y=0$ and 4. However, in the boundary of the various clusters, Si atoms are bound to O and Si, thus forming intermediate tetrahedra. We can therefore schematically describe the phase-separated SiO as composed of spherical clusters of pure silicon with average radius a embedded in a SiO_2 matrix. Hence, on a purely geometric standpoint, three kinds of Si atoms can be defined by a SiO volume unit: (1) Si in the pure silicon clusters, (2) Si in the boundary of the clusters (region of thickness b), and (3) Si in the silica matrix. Given N_1 and N_2, the values of the silicon atomic concentrations in the Si clusters and in the SiO_x boundary regions, respectively, the relative weights W of the oxidation states given by the XPS measurements can be written

$$W(\mathrm{Si}^0)=\tfrac{4}{3}\pi a^3 n_0 N_1 ,$$

$$W(\mathrm{Si}^{2+})+W(\mathrm{Si}^{3+})=4\pi a^2 b n_0 N_2 ,$$

n_0 being the number of Si clusters per volume unit. In the case of the RTA sample, which is the most phase separated, one can give a very crude approximation of the size of the Si clusters: Considering that the boundary zone is essentially composed of Si_2O_3 (see Fig. 7) with a thickness b equal to about 0.4 nm (of the order of the intermediate transition region at the Si–thermal-SiO_2 interface), and taking densities equal, respectively, to 2.33 and 2.2 for Si and SiO_x, one obtains

$$a\sim 4 \text{ nm} .$$

Although this value is only indicative, there is a great difference with the size of the Si crystalline areas observed by RHEED, i.e., the crystalline areas represent only a very small part of Si clusters.

As discussed above no change in the stoichiometry can be detected by RBS. If the upper layers were rather SiO_2 than SiO they could not extend over more than ~ 4 nm from the surface. The fitting procedure allows us to estimate the stoichiometry if one assumes that the sample has a constant oxygen concentration up to the surface. If $W(\mathrm{Si}^{n+})$ is the weight of the nth oxidation state, and x the O-to-Si ratio (SiO_x), one can write

$$x=\tfrac{1}{2}\sum_{n=1}^{4} nW(\mathrm{Si}^{n+}) ,$$

assuming that every oxygen is a bridging oxygen (Si—O—Si). The calculated values of x are given in Table I. For each sample a value greater than unity is found. Hence, taking into account the RBS results, the oxygen concentration is likely to increase for the layers very close to the surface. If one assumes that the top surface layers of the samples are pure SiO_2 with an abrupt transition with underlying SiO_1 layers, which is probably unrealistic, one can estimate with this working hypothesis the thickness of this topmost SiO_2 layer. Taking the mean free paths of the photoelectrons around 2.7 nm both in SiO_1 and SiO_2 and similar densities (~ 2.2 g/cm^3) for both materials[8] one obtains SiO_2 thicknesses not exceeding 3.5 nm, i.e., not detectable by RBS.

O 1s core levels

O 1s lines can be fitted by a single Gaussian: The positions E_B and half-widths at half maximum Γ for each sample are given in Table II. For the test sample, the width of the O 1s line and the anomalous energy difference $\Delta E_B(\mathrm{Si}^{4+}-\mathrm{O}\ 1s)$ [typically 429.7–429.8 eV (Refs. 20 and 23)], can be explained by the presence of extra lines associated to oxygen in the suboxides. Γ is smaller in crystalline forms of silica or in thick thermal silica films on silicon (typically 0.65 eV in the same experimental conditions). Indeed, for very thin films of thermal silica (less than 2 nm), Γ is comparable to that of the RTA sample (i.e., 0.75 eV).[20] This broadening of the O 1s levels may be indicative of a larger disorder in Si—O bond lengths and Si—O—Si bond angles than in thick thermal a-SiO_2 or in c-SiO_2, and may be due to the special structure of the films (voids, impurities, etc.).

Valence-band spectra

The valence-band and O 2s spectra after background subtraction for the test, plasma, RTA, and laser samples are shown in Fig. 8. The energy position of the O 2s peak maximum remains unchanged for all the samples, indicating the absence of any charging effects. As in the case of vitreous or crystalline SiO_2,[24] three groups of structure are clearly distinguishable. At the top of the valence band, an O 2p lone-pair band (group I) is followed at higher binding energies, by two bonding bands with Si 3p–O 2p character (group II) and Si 3s–O 2p character (group III). In Fig. 8 we denote by I, II, III these three groups, whose positions do not vary appreciably before and after treatment.

TABLE II. Binding energies (E_B), O 1s–Si^{4+} energy difference ΔE_B (O 1s–Si^{4+}) and half-width at half maximum (Γ).

Sample	Test	Plasma	RTA	Laser
E_B (eV)	532.75	533.1	533.1	532.95
ΔE_B (O 1s–Si^{4+}) (eV)	429.25	429.6	429.6	429.55
Γ (eV)	0.85	0.80	0.75	0.80

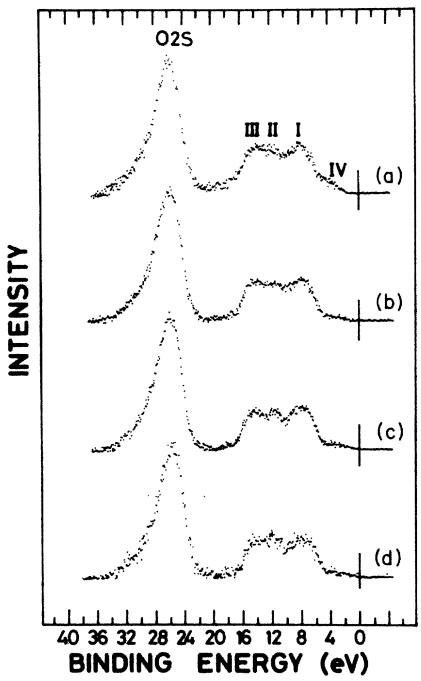

FIG. 8. Valence-band and O $2\dot{s}$ spectra obtained for the (a) test sample, (b) plasma sample, (c) RTA sample, and (d) laser sample. The zero energy is taken at the Fermi level.

An additional group, (denoted IV) is found lying in the band gap of bulk silica. This group is due to Si—Si bonds which give states at these energies.[25] After plasma, RTA, or laser treatments, group IV broadens while its maximum decreases. New states are thus *populated closer to the Fermi level.* The dip between group I and groups II and III is more visible on the RTA and laser samples than on the samples kept at room T, i.e., the test and plasma samples. This may be indicative of a greater ordering of the oxide network[26] when the samples are treated at high T. It could also be connected to the observed distinct oxygen stretching frequencies of high-T and low-T silica, in the ir absorption spectra.

DISCUSSION

RHEED and XPS experiments yield complementary information: The former is sensitive to long-range order, the latter to short-range order, bonding configurations, and dielectric response of the material. As indicated by RHEED the matrix is amorphous. Microcrystallites of silicon (and silica) dispersed in this amorphous matrix appear after treatment, even for the plasma treatment performed at room T. The energy pinning of the Si $2p$ oxidation states suggests that the dielectric properties of the oxide matrix are not much affected by the various treatments. However, as indicated above, after treatment both the Si^0 states move towards lower binding energies, while the broadening of the Si states of the valence band is observed. These two points can be related to Si cluster growth. In fact, an increase in the interaction between silicon orbitals can explain the broadening of group IV: This could mean that the probability that a given Si is surrounded by other Si atoms has increased after treatment, i.e., that Si clusters grow at the expense of suboxide configurations. The shift of Si^0 states towards lower binding energy can be explained by a modification in the way a Si core hole is screened. When Si clusters are very small, screening is essentially provided by the polarization of the neighboring atoms. When the clusters become larger, the delocalized electrons of the valence band now screen the core hole. Size effects have already been related to core level shifts and valence-band spectra modifications of metallic clusters deposited on insulators (alkali halides),[27] or on a poorly conducting substrate (*a*-carbon).[28,29] The valence bands of small clusters were greatly narrowed relative to the spectrum of the bulk material, probably in relation to the decrease in coordination number. Related to this, a shift of the metal, core levels towards higher binding energy was also observed, when the size of the metal clusters was reduced. For metals, the change in the way core photohole screening is achieved occurs for cluster diameters r greater than 1 nm, after which the binding energies reach the bulk values with a $\sim 1/r$ dependence.[28] Of course, in this study we have no precise values for the size of the growing Si clusters but we believe they are to be distinguished from the Si microcrystals (of size 10–100 nm), dispersed in the oxide matrix, that are observed in RHEED. If locally a certain critical size of Si clusters is exceeded, the growth of Si microcrystallites may then occur.

A microscopic description of the phenomena leading to Si cluster growth can be searched for in the following way. In the test SiO film isolated Si–Si bonds giving rise to intermediate oxidation states (Si^{3+}) can be considered as the precursors of mobile oxygen vacancies. Two sp_3 silicon hybrids can interact to give a filled bonding σ state and an empty antibonding σ^* state. The energy splitting between σ and σ^* ranges from ~ 4 eV (weak bond) to 7.7 eV (strong bond),[30] depending on the degree of relaxation of the surrounding lattice. Isolated Si—Si bonds can lose one bonding electron, for example by $\sigma \rightarrow \sigma^*$ transitions under light excitation followed by delocalization of the promoted electron in a conduction-like band. This can also occur by transferring an electron (tunneling or thermally activated process) from a σ state to a nonoccupied state of the Si cluster valence band. The size of the clusters already present needs to be large enough to create valence and conduction bands. The resulting localized one-electron Si—Si bond is unstable, and breaks[31] to give one neutral Si_3^0 (E' center) and one positive charged Si_3^+ defect (the superscript being the charge of the defect in the covalent limit, and the subscript the number of oxygen first neighbors). Si_3^+ (an oxygen half-vacancy), or more precisely O_3^+, its more stable derivative after reaction with a bridging oxygen, is capable of motion.[31,32] The gain in stability of O_3^+ relative to Si^{3+} is $\sim 1-1.9$ eV, and thus corresponds to the energy barrier for motion.[31] From the observation in various SiO_x materials, of Si clusters growing upon heating, Nesbit[33] has extracted an activation energy of the Si diffusion coefficient equal to 1.9 eV (including both defect creation and motion energy).

Remarkably, not only can SiO disproportionate under heating at high temperature or under uv laser irradiation (leading also to heating), it can do so under the influence of an electronic flux, at room T, during the plasma treatment. If, in purely thermal treatments, hole trapping on a Si—Si isolated bond can be a likely process leading to bond breaking, it should be accelerated by irradiation in the uv range (here the photon energy was 6.4 eV). Indeed the largest shift towards lower binding energies was obtained for the uv laser sample.

The most puzzling question to be addressed is the case of transformations at room T under plasma treatments. As the surface potential differs from the plasma potential, by a few eV, and since the electrons injected in the SiO film are further accelerated by the large electric field (3×10^6 V/cm), some of them could have energy sufficient to create the holes that can in turn break the isolated Si—Si bonds. Moreover the motion of positively charged oxygen half-vacancies should be highly directed by the field normal to the sample surface. The XPS results do not seem to indicate that silicon has accumulated near the top surface. In contrast, RHEED results suggest that Si microcrystals are preferentially found near the surface. Cross-sectional microscopy should be a help to check if the electric field induces inhomogeneity with depth.

CONCLUSION

Studying the transformation of an a-SiO thin film under room-temperature plasma treatment, heating, and uv irradiation in a nonoxidizing atmosphere, we have shown that the as-deposited oxide, not a mixture of Si and SiO_2, is subject to disproportionation into the latter compounds. This is shown by the shift of the ir absorption line of the oxygen stretching mode. This is also clearly evidenced by the changes in the XPS core-level Si $2p$ spectra that display a strong decrease in intermediary Si suboxide states after treatment. The growth of Si clusters can also explain the Si^0 states shift towards lower binding energy as well as the changes in the valence-band spectra. We believe that these clusters precede the local growth of Si microcrystallites dispersed in a still-amorphous matrix, as observed by RHEED.

We show that at room T the effects of the large flow of electrons provided by the plasma can be compared to the effects of thermal processes.

Focusing on the instability of Si—Si bonds (Si^{3+} states) in an amorphous oxide matrix, this study can help the understanding of both SiO and c-Si oxidation mechanisms under various oxidation processes.

ACKNOWLEDGMENTS

The authors wish to express their thanks to A. Laurent and J. P. Enard for their help during experiments. This work was supported by the Centre National de la Recherche Scientifique (Greco No. 86].

[1]S. E. Blum, K. H. Brown, and R. Srinivasan, Appl. Phys. Lett. **43**, 1026 (1983).
[2]C. R. M. Grovenor, A. Cerezo, and G. D. Smith, Mater. Res. Soc. Symp. Proc. **37**, 199 (1985).
[3]A. M. Stoneham, C. R. M. Grovenor, and A. Cerezo, Philos. Mag. B **55**, 201 (1987).
[4]J. Perriere, B. Pelloie, E. Fogarassy, and A. Slaoui, Appl. Surf. Sci. **29**, 433 (1987).
[5]E. Fogarassy, J. L. Regolini, C. Fuchs, and A. Grob, Eur. Mater. Res. Soc. Symp. Proc. **12**, 255 (1986).
[6]E. Fogarassy, S. Unamuno, J. L. Regolini, and C. Fuchs, Philos. Mag. B **55**, 253 (1987).
[7]H. R. Philipp, J. Phys. Chem. Solids **32**, 1935 (1971).
[8]G. Hollinger, thesis, Université Claude Bernard, Lyon I, 1979.
[9]J. Perriere, J. Siejka, A. Laurent, J. P. Enard, and F. d'Heurle, in *Plasma Synthesis and Etching of Electronic Materials*, edited by R. P. H. Chang and B. Abeles, Vol. 38 of *MRS Symposia Proceedings*, (Materials Research Society, Pittsburgh, 1985), p. 443.
[10]R. Nyholm and N. Mårtensson, Chem. Phys. Lett. **74**, 337 (1980).
[11]D. A. Shirley, Phys. Rev. B **5**, 4709 (1972).
[12]W. K. Chu, J. W. Mayer, M. A. Nicolet, T. M. Buck, G. Amsel, and F. Eisen, Thin Solid Films **17**, 1 (1973).
[13]N. Fuschillo, M. Gimpl, and A. McMaster, J. Appl. Phys. **36**, 575 (1965).
[14]S. S. Chao, G. Lucovsky, S. Y. Lin, C. K. Wong, P. D. Richard, D. V. Tsu, Y. Tagaki, J. E. Keem, J. E. Tyler, and P. P. Pai, J. Non-cryst. Solids **77-78**, 929 (1985).
[15]W. A. Pliskin and H. S. Lehmann, J. Electrochem. Soc. **112**, 1015 (1965).
[16]G. Hollinger and F. J. Himpsel, Phys. Rev. B **28**, 3651 (1983).
[17]G. Hollinger, J. F. Morar, F. J. Himpsel, G. L. Hughes, and J. L. Jordan, Surf. Sci. **168**, 609 (1986).
[18]W. Braun and H. Kuhlenbeck, Surf. Sci. **180**, 279 (1987).
[19]F. J. Grunthaner, P. J. Grunthaner, M. H. Hetch and D. Lawson, *Proceedings of the INFOS 85 Conference, Toulouse, France, 1985* (North-Holland, Amsterdam, 1985), pp. 1–10.
[20]F. Rochet, S. Rigo, M. Froment, C. d'Anterroches, C. Maillot, H. Roulet, and G. Dufour, Adv. Phys. **35**, 237 (1986).
[21]G. Hollinger, Y. Jugnet, P. Pertosa, and Tran Minh Duc, Chem. Phys. Lett. **36**, 441 (1975).
[22]L. Ley, J. Reichardt, and R. L. Johnson, Phys. Rev. Lett. **49**, 1664 (1982).
[23]A. Iqbal, C. W. Bates and J. W. Allen, Appl. Phys. Lett. **47**, 1064 (1985).
[24]J. Chelikowsky and M. Schluter, Phys. Rev. B **15**, 4020 (1977).
[25]J. Robertson, Philos Mag. B **51**, 183 (1985).
[26]M. Brodsky and M. Cardona, J. Non-Cryst. Solids **31**, 81 (1978).
[27]H. Roulet, J. M. Mariot, G. Dufour, and C. F. Hague, J. Phys. F **10**, 1025 (1980).

[28]S. B. Di Cenzo and G. K. Wertheim, Comments Solid State Phys. **11**, 203 (1985).
[29]G. K. Wertheim, Z. Phys. B **66**, 53 (1987).
[30]E. P. O'Reilly and J. Robertson, Phys. Rev. B **27**, 3780 (1983).
[31]J. Robertson, Philos. Mag. B **55**, 673 (1987).
[32]F. Rochet, B. Agius, and S. Rigo, J. Electrochem. Soc. **131**, 914 (1984).
[33]L. A. Nesbit, Appl. Phys. Lett. **46**, 38 (1985).

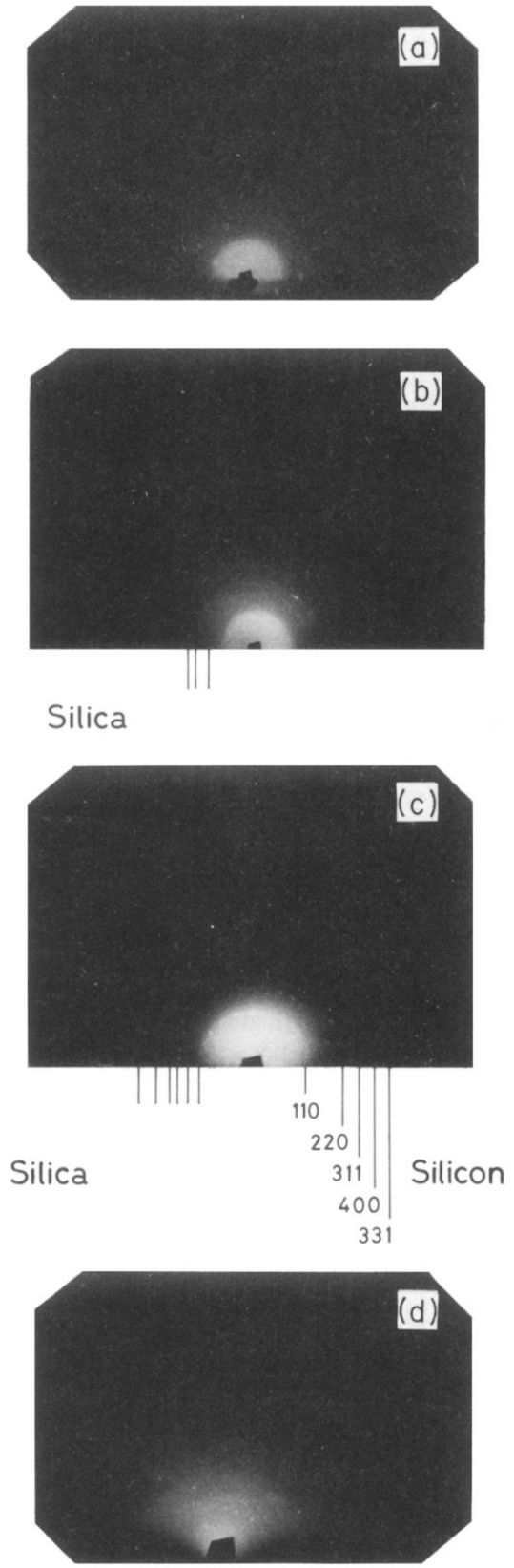

FIG. 3. Electron diffraction patterns observed by reflection (RHEED): (a) plasma sample (surface observation), (b) plasma sample (in-depth observation), (c) RTA sample, (d) Laser sample. Bright points distributed on rings corresponding to *c*-Si interreticular distances are seen in (a)–(d). Rings indicative of an ordered SiO_2 phase are seen in (b) and (c).